Meteorological observations on Mount Everest in 2005*

Xie Aihong[1**], Qin Dahe[1], Ren Jiawen[1], Qin Xiang[1], Xiao Cunde[1,2], Hou Shugui[1], Kang Shichang[1,3], Yang Xingguo[1,4] and Jiang Youyan[1]

(1. Key Laboratory of Cryosphere and Environment, Cold and Arid Regions Environment and Engineering Research Institute, Chinese Academy of Sciences, Lanzhou 730000, China; 2. Chinese Academy of Meteorological Science, Beijing 100081, China; 3. Institute of Tibetan Plateau Research, Chinese Academy of Sciences, Beijing 100085, China; 4. Gansu Provincial Meteorological Bureau, Lanzhou 730000, China)

Accepted on January 8, 2007

Abstract Mount Everest, the highest point on the Earth is often referred to as the earth's third pole as such the place is relatively inaccessible and little is known about its meteorology. In April 2005, an automatic weather station was installed at the mountain's North Col (6523 m a.s.l.). According to the observational 10-minute mean and daily records, the meteorological characteristics were analyzed. All the meteorological elements displayed obvious diurnal variations during May 1 to July 22, 2005. The monthly variation of daily meteorological elements on Mount Everest coincided with that on Dingri, the closest routine meteorological station, with the high correlation coefficients of 0.928, 0.877, 0.682, 0.755, 0.826 and 0.676 ($n = 83$, $p < 0.001$) for mean temperature, minimum temperature, maximum temperature, relative humidity, pressure and wind speed, respectively. Furthermore, the vertical mean gradient of temperature was above 0.6℃/100 m, especially for the daily maximum temperature. Most weather events on Mount Everest prominently appeared on the same day as those on Dingri, especially those from daily mean pressure, temperature and relative humidity with the cross-correlation coefficients of 0.673, 0.485 and 0.487 ($n = 83$, $p < 0.001$), respectively. Some other weather events on Mount Everest lagged one-day behind those on Dingri. Furthermore, forecasting of the weather events on Mount Everest from pressure on Dingri was more reliable than those from the other meteorological elements. The conclusions are much important for research on meteorology and climate changes in the region.

Keywords: Mount Everest, meteorological observation, Dingri County, radiation, air temperature, relative humidity, air pressure, wind.

The Himalayas at the southern edge of the Tibetan Plateau is uniquely placed to modulate the regional monsoon climate in India, Nepal and the Tibetan Plateau of China[1]. Within the Asian monsoon system, it is well recognized that the Himalayas and Tibetan Plateau exert a profound thermal and dynamical influence on the atmospheric circulation, involving a strong interaction between the land, atmosphere and ocean[2]. Mount Everest (27°59′ N, 86°55′ E) lies in the central Himalayas and is often referred to as the earth's "third" pole, at an elevation of 8844.43 m (as promulgated by the State Council Information Office, People's Republic of China in October 2005, 3.7 m lower than 8848.13 m measured in 1975). For a few centuries, Mount Everest has been the subject of exploration for both scientific and recreational purposes[3,4], and most researches focused on the impact of the low barometric pressure on human physiology and performance[5,6]. Chinese Academy of Sciences and General Administration of Sport of China organized three integrated scientific expeditions to Mount Everest region during 1959 to 1960, 1966 to 1968 and in 1975, respectively[7,8]. Since 1993, the "Pyramid" meteorological observatory has been established at an elevation of 5050 m on the southern slope of Mount Everest[2,9]. In 1998, a portable weather station was operated at Mount Everest's South Col (7986 m a.s.l.) for 4 months[10]. There were also some studies on summer monsoon onset and valley diurnal winds on the south-facing slope in the Mount Everest region[4,11—13]. However, due to the difficult logistics supply in the extreme high elevation regions on Mount Everest, the observational meteorological data are still very scarce. Therefore, many researchers studied climate changes through proxies (such as ice cores) from the regional glaciers[14—19]. Field investigation and observation on the glacier's terminus position between 1966 and 2004 showed

* Supported by National Natural Science Foundation of China (Grant Nos. 40501015 and 90411003), and the Knowledge Innovation Program of the Chinese Academy of Sciences (Grant No. KZCX3-SW-344)

** To whom correspondence should be addressed. E-mail: xieaih@lzb.ac.cn

that, for East Rongbuk glacier (28°02′ N, 86°57′ E, 12.8 km in length, 46.27 km^2 in area), the largest glacier on the northern slope of Mount Everest, snow line accelerated upward and the retreat of the glacier was speeding up somewhat at a rate of 5.5, 7.6, 8.0, 8.3 m per year during 1966 and 1997, 1997 and 1999, 1999 and 2002, 2002 and 2004, respectively[15,16].

Although these efforts have contributed to our knowledge of the meteorology and climate in the region, there is still a pressing need for meteorological data from the high elevation regions. In an attempt to satisfy this demand, an automatic weather station (AWS) was installed on East Rongbuk glacier of Mount Everest in April 2005, at a height of 6523 m a.s.l (Fig. 1). We believe that this is one of the highest sites for AWSs where continuous meteorological data have ever been collected and thus are valuable datasets with which the meteorology of the high elevation in Himalayas region was investigated. This research mainly aimed at the documentation of the diurnal and monthly variability of the meteorological feature in the extreme high elevation under the condition of global warming[20, 21] and the regional glaciers accelerating retreat[15,16], and filling the gap of research above 6500 m a.s.l. on the northern slope of Mount Everest from a meteorological perspective.

1 Data

On April 27, 2005, an AWS was installed at Ruopula Pass of East Rongbuk glacier, less than 5 km northeast of the peak of Mount Everest (Fig. 1). The landform was gentle in incline, covered with thick snow and firn ice below snow surface, and steep precipices stood on both sides a few hundred meters away. The AWS was located the highest at the saddle-like pass (28°01′0.95″ N, 86°57′48.4″ E, 6523 m a.s.l.).

The specification of sensors in the AWS (with CR1000 measurement and control system) is given in Table 1. The AWS recorded the meteorological data continuously every 10 minutes (10-minute average) and every 24 hours (daily minimum and maximum) from 14:20 LST (Local Standard Time or Beijing Time) April 30 to 10:40 LST July 23, 2005. From July 23 to October 17, 2005, the meteorological data were discontinuous. Therefore, this paper covers meteorological data from May 1 to July 22, 2005 on Mount Everest.

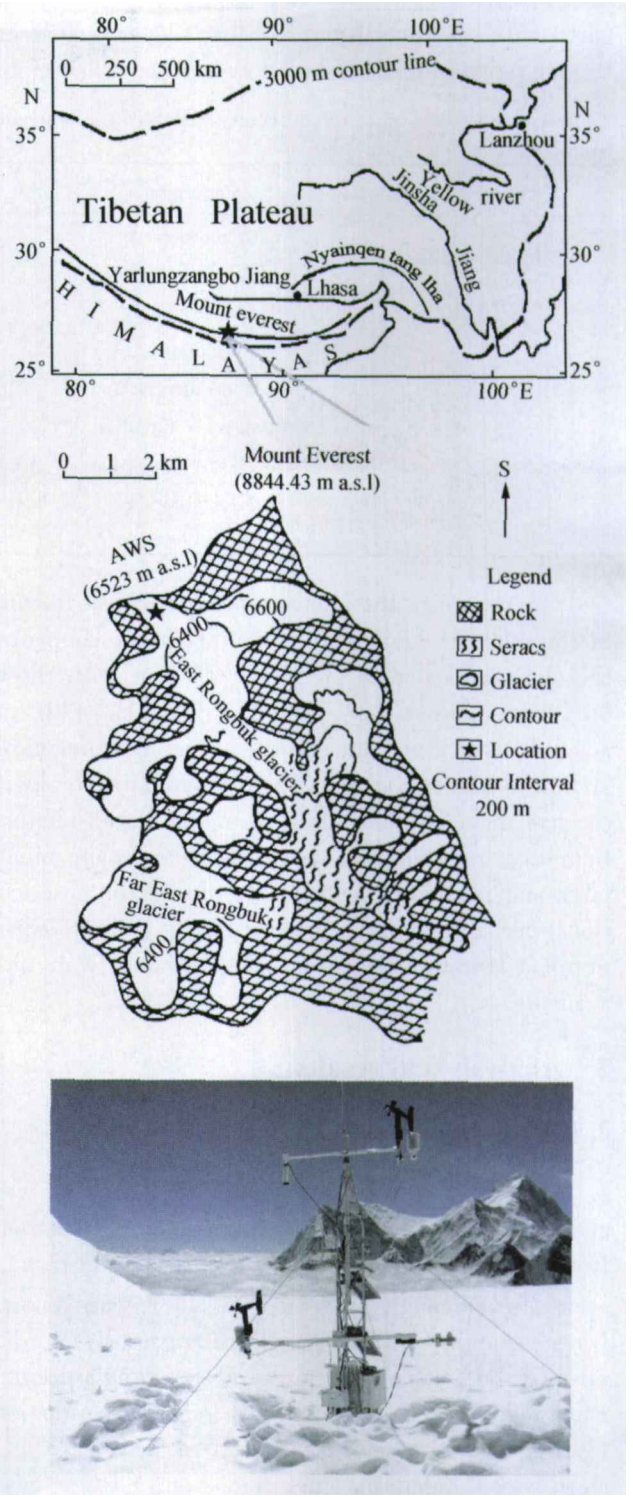

Fig. 1. Location map for the automatic weather station (AWS) on Mount Everest. The pentagon represents the AWS location.

The AWS had one layer of actinograph and barometer, and two layers of hygrothermographs, anemometers and dogvanes. Moreover, the height above snow surface for the two layers varied with snow depth. When the AWS was installed on April 27, the height was 1.5 m and 2.5 m, respectively. When the AWS was dismantled on October 17, the height was 0.3 m and 1.3 m, respectively. Com-

pared with the upper layer, the lower layer was closer to and more influenced by snow surface. Therefore this study analyzed the observational data in the upper layer only.

Table 1. Specification of the different sensors in the automatic weather station (AWS) installed on North Col of Mount Everest from May 1 to July 22 in 2005

Sensor type	Parameter	Accuracy	Range
Model 41382	Air temperature	±0.3	−50 to 50℃ or −50 to 150℉
	Relative humidity	±2%	0 to 100%
PTB210	Air pressure	±0.50 hPa	50 to 1300 hPa (−40℃ < T < 60℃)
YOUNG 05103	Wind speed	±0.3 $m \cdot s^{-1}$	0 to 60 $m \cdot s^{-1}$ (Max is 100 $m \cdot s^{-1}$)
	Wind direction	±3 deg	0 deg to 355 deg (5 deg open)
CNR 1	Long-wave radiation	±3%	0.305 μm < λ < 2.8 μm
	Short-wave radiation	±3%	5 μm < λ < 50 μm
	Net radiation	From ±3% to ±10%	Calculated from the long-wave and short-wave radiation

To recognize the monthly meteorological feature in the extreme high mountain, this paper compares the observational data on Mount Everest with those on Dingri County (28°38′ N, 87°05′ E, 4301 m a.s.l.), which was the closest routine meteorological station to Mount Everest. The compared meteorological data included daily mean of temperature, relative humidity, pressure and wind speed, and daily minimum and maximum temperature during the observational period. While the corresponding data of radiation and 10-minute mean on Dingri County were unavailable.

2 Analysis and results

2.1 Radiation

The mean diurnal variation (Fig. 2(a)) was characterized by one peak for all kinds of radiation from May 1 to July 22 in 2005. With the Sun rising, solar altitude angle increased[22], downward short-wave radiation (DR) strengthened apparently, so did upward short-wave radiation (UR), downward long-wave radiation (DLR), upward long-wave radiation (ULR). As the calculated result of long-wave and short-wave radiation, net radiation (RN) also strengthened after sunrise. It got to its maximum at noon or in the afternoon, then decreased and kept low during night for DR, UR, RN, ULR and DLR. For the mean diurnal variation, DR and UR changed much, RN changed little with a positive value in daytime and a negative value in nighttime, and DLR and ULR varied least.

From May 1 to July 22, the Sun moved northward[22], solar altitude angle increased, plateau monsoon and Indian summer monsoon started to control the region gradually[10,13,23], precipitation increased and cloud strengthened[24]. Therefore, DLR and ULR enhanced, DR and UR weakened, and RN changed little with slight increase during the observational period (Fig. 2(b)). The characteristic of diur-

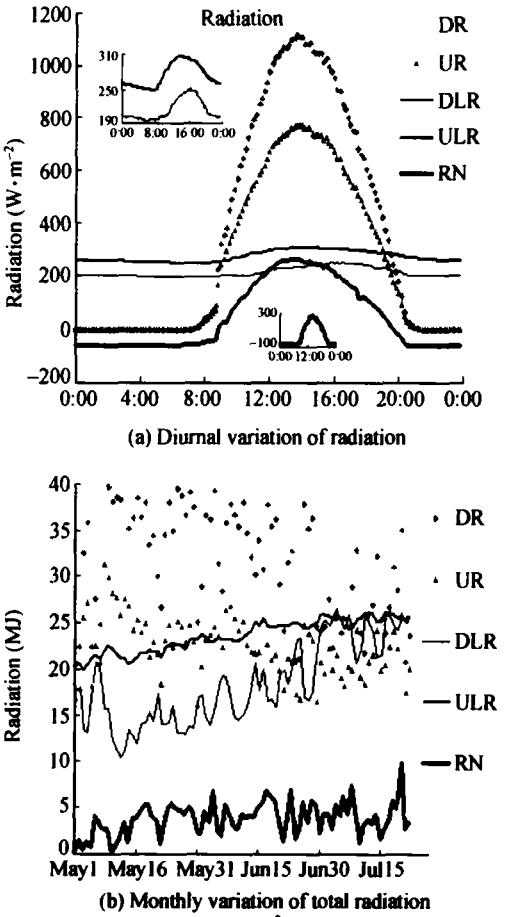

Fig. 2. Diurnal variation ($W \cdot m^{-2}$) and monthly variation (MJ) of radiation on Mount Everest observational site (6523 m a.s.l) from May 1 to July 22 in 2005. DR stands for downward short-wave radiation, UR for upward short-wave radiation, DLR for downward long-wave radiation, ULR for upward long-wave radiation, and RN stands for net radiation.

nal and monthly variation coincides with that on the western Tibetan Plateau[24].

2.2 Air temperature

The diurnal variation of air temperature (Fig. 3) was characterized by one peak and one vale. After the Sun rising, solar altitude angle increased[22], solar radiation strengthened (Fig. 2(a)), sensible and latent heat transferred from the snow surface, air temperature increased abruptly after sunrise, and got to its peak at noon, then decreased and reached its minimum before sunrise. The one-peak-and-one-vale character coincided with that on large scale[22], and was consistent with the research result of Ye et al.[23] for Mount Everest.

From May 1 to July 22 in 2005, the Sun moved northward, solar altitude angle increased[22], air temperature (Fig. 4(a)) increased slowly with large rebounding in early and middle May, strengthened abruptly from late May to middle June, and kept high from late June to July, during which the most prominent was the abrupt increasing in late May and middle June. With the 10-minute mean temperature increasing, the daily minimum and maximum increased simultaneously (Fig. 4(a)), with a high cross-correlation coefficients of 0.906 and 0.894 ($n = 83$, $p < 0.001$), respectively.

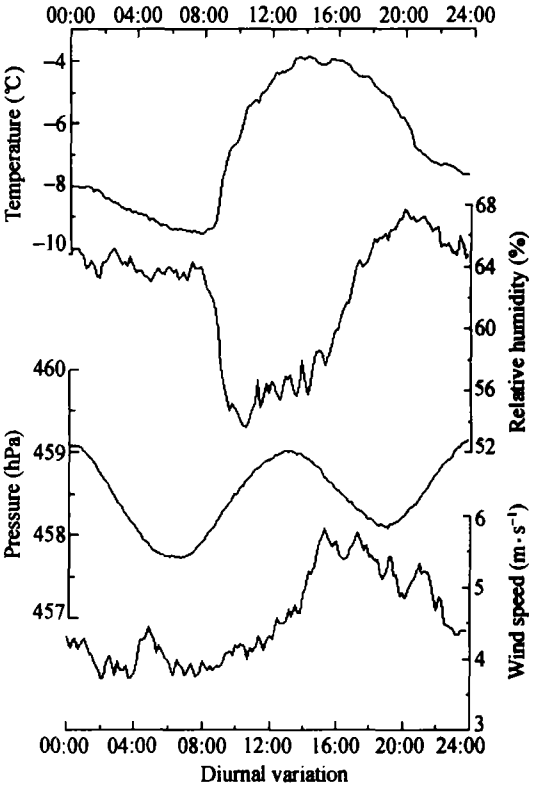

Fig. 3. Diurnal variation of air temperature (℃), relative humidity (%), air pressure (hPa) and wind speed ($m \cdot s^{-1}$) on Mount Everest (6523 m a.s.l) from May 1 to July 22 in 2005.

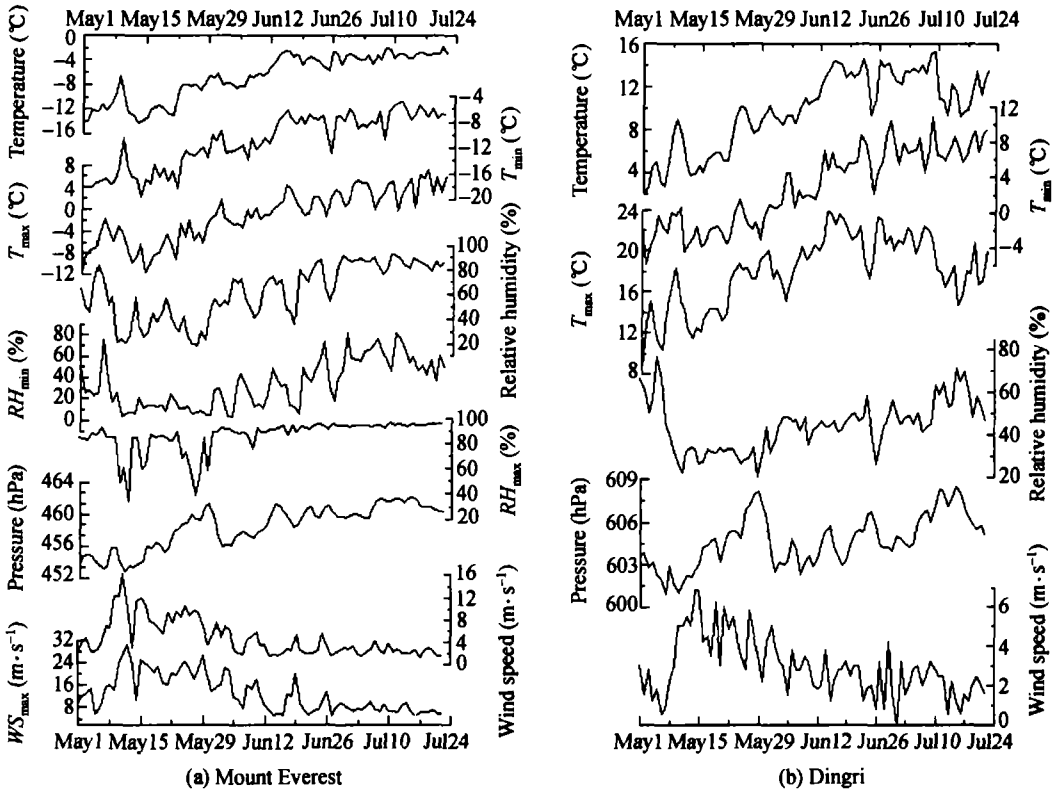

Fig. 4. Monthly variation of daily meteorological elements on Mount Everest (6523 m a.s.l) (a) and Dingri County (b) from May 1 to July 22 in 2005. T_{max} stands for daily maximum temperature (℃), T_{min} for daily minimum temperature (℃), RH_{max} for daily maximum relative humidity (%), RH_{min} for daily minimum relative humidity (%) and WS_{max} for daily maximum wind speed ($m \cdot s^{-1}$). Temperature (℃), relative humidity (%), pressure (hPa) and wind speed ($m \cdot s^{-1}$) represent daily mean of the corresponding values.

The monthly variation of temperature on Mount Everest coincided with that on Dingri (Fig. 4(b)), with the correlation coefficients of 0.928, 0.877 and 0.682 ($n = 83$, $p < 0.001$) for daily mean, minimum and maximum temperature, respectively. For the daily mean, minimum and maximum temperature during May 1 to July 22, the vertical mean gradient between Mount Everest observational site (6523 m a.s.l) and Dingri County (4301 m a.s.l) was 0.75℃/100 m, 0.63℃/100 m, and 0.82℃/100 m, respectively. The vertical maximum gradient was 0.85℃/100 m, 0.83℃/100 m and 1.18℃/100 m, respectively. The vertical minimum gradient was 0.55℃/100 m, 0.43℃/100 m and 0.43℃/100 m, respectively. Therefore, the vertical temperature gradient was above the normal 0.6℃/100 m, especially for the daily maximum temperature. For the anomalously maximum temperature on Dingri, it may be due to the surrounding human activities, error in reading data and decrease of daily maximum temperature from the lower layer to the upper layer according to the law of exponent/logarithm[25].

The cross-correlation refers to the correlation between variables in one time series and the corresponding variables in the other time series[26]. In this paper, the cross-correlation analysis suggests that the weather events from daily mean temperature (Fig. 5 (a)) on Mount Everest prominently appeared on the same day ($r = 0.485$, $n = 83$, $p < 0.001$) as those

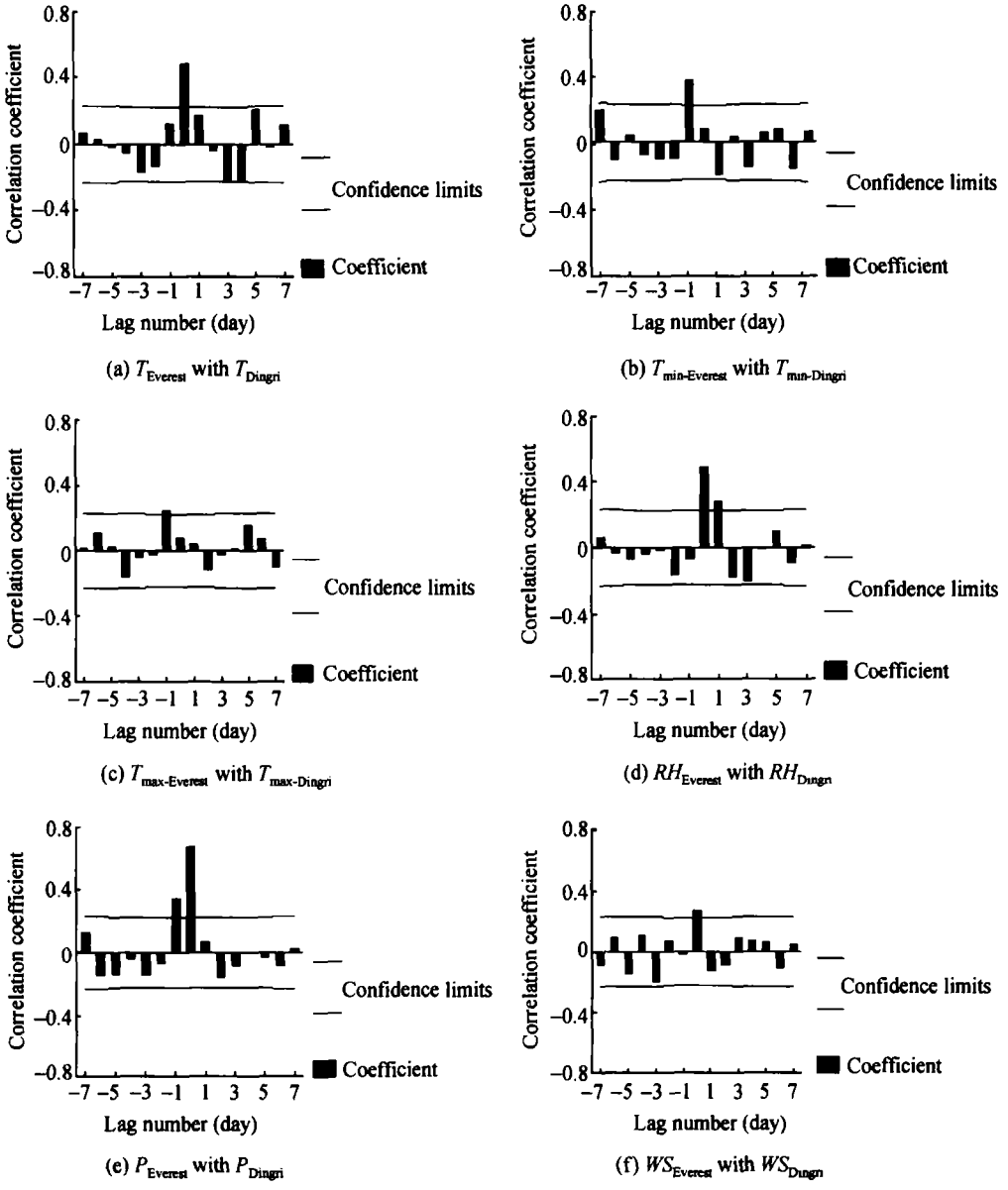

Fig. 5. Cross-correlation plots of observational data between Mount Everest and Dingri for (a) daily mean temperature (℃), (b) daily minimum temperature (℃), (c) daily maximum temperature (℃), (d) daily mean relative humidity (%), (e) daily mean air pressure (hPa) and (f) daily mean wind speed from May 1 to July 22 in 2005. The red rectangles indicate the cross-correlation coefficient, and the black lines represent the confidence limits.

on Dingri. However, for the daily minimum and maximum temperature (Fig. 5(b)), the weather events on Mount Everest often lagged one day behind those on Dingri with the cross-correlation coefficients of 0.366 ($n = 83$, $p < 0.001$) and 0.245 ($n = 83$, $p = 0.05$), respectively.

2.3 Relative humidity

Diurnal variation of relative humidity had an obvious feature of single vale (Fig. 3). It began to decrease abruptly after 08:00 LST, and reached its minimum and maximum during sunrise and sunset, respectively. The increasing of relative humidity in the afternoon near the snow surface was mostly due to the daytime mountain-vale wind convergent into the Plateau interior in summer resulting from heating effect of the Tibetan Plateau[14,23], more southerly occurring in the afternoon (Fig. 5(d)) and bringing plenty of water vapor from the Indian monsoon in June and July, and surface snow sublimating in the afternoon under the heating from solar radiation enhancing (Fig. 2(a)).

In May, Mount Everest region was controlled by the westerly circulation and influenced by airflow from the arid and semi-arid regions. In June, the Plateau summer monsoon began in the southern plateau[2,9,12,23], then Indian summer monsoon advanced northward with plenty of water vapor[12,14,23]. In July, Plateau summer monsoon and Indian summer monsoon developed into maturation, and dominated Mount Everest. Wherefore, relative humidity (Fig. 4(a)) was low in middle and late May with much fluctuation, increased rapidly with rebounding in June, and almost kept high in July.

The monthly variation of relative humidity on Mount Everest coincided with that on Dingri (Fig. 4(b)), with the correlation coefficients of 0.755 ($n = 83$, $p < 0.001$). The cross-correlation analysis suggested that the weather events from daily mean relative humidity (Fig. 5(d)) on Mount Everest prominently appeared on the same day ($r = 0.487$, $n = 83$, $p < 0.001$) as those on Dingri, and some occurred one day ahead of those on Dingri ($r = 0.275$, $n = 83$, $p = 0.02$).

2.4 Air pressure

The diurnal variation of air pressure on Mount Everest (Fig. 4(a)) displayed twin peaks and twin vales. Twin peaks occurred at midnight and at noon, and twin vales appeared before sunrise and during sunset. Because of the seasonal variation of heating field on planetary scale, the 700 hPa geopotential height was a compartmental layer in Mount Everest region, above which pressure increased with temperature rising, and *vice versa*. At the observational site (450 hPa to 47 hPa), pressure varied with temperature in a positive phase, which reached the minimum before sunrise and maximum during noon, respectively. The other peak and vale of diurnal variation was due to the maximum belt of positive increasing pressure at high altitude around the Tibetan Plateau, which suggested that pressure was higher at 20:00 LST than at 08:00 LST, and strengthened with height resulting from the mountain-vale wind on a large scale[23].

Daily mean pressure on Mount Everest increased with temperature rising from May to July (Fig. 4(a)), especially in late May, which resulted from the seasonal variation of heating field on planetary scale, just as the diurnal variation of pressure. Because of the seasonal variation for heating field on local scale, pressure decreased with temperature decreasing in early June.

The monthly variation coincided with that on Dingri (Fig. 4(b)) with a correlation coefficient of 0.826 ($n = 83$, $p < 0.001$). The cross-correlation analysis suggested that the weather events from daily mean pressure (Fig. 5(e)) on Mount Everest prominently appeared on the same day as those on Dingri with a high cross-correlation coefficient of 0.673 ($n = 83$, $p < 0.001$), and some occurred one-day lag behind those on Dingri ($r = 0.341$, $n = 83$, $p = 0.01$).

2.5 Wind

The mean diurnal variation of wind speed was characterized by one peak with asymmetry during day and night (Fig. 3). Wind speed increased abruptly at noon, reached its maximum in the afternoon, and changed little during night to the next morning, which was consistent with the research result of Egger in the southern flank of Mount Everest[4,11]. The more heating strengthened in the Plateau, the more aerodynamic instability was, and the more air from upper level flew downward[23], and the more wind speed intensified. From May 1 to July 22 in 2005, 10-minute mean wind speed (Fig. 4(a)) was weak in

early May, then enhanced abruptly, reached its maximum on May 11, and decreased with fluctuation during late May to July. Daily maximal wind speed varied with the daily mean wind speed with a correlation coefficient of 0.792 ($n=83$, $p<0.001$). The monthly variation of mean wind speed coincided with that on Dingri (Fig. 4(b)) with a correlation coefficient of 0.676 ($n=83$, $p<0.001$). The cross-correlation analysis suggested that the weather events from daily mean wind speed (Fig. 5(f)) on Mount Everest often appeared on the same day as those on Dingri with a cross-correlation coefficient of 0.268 ($n=83$, $p=0.02$).

The diurnal and monthly variations of wind direction are indicated in Fig. 6(a) and 6(b), respectively. In May, Mount Everest area was mostly controlled by the westerly circulation, northerly and north-north-westerly predominated (Fig. 6), and southerly was little and happened in the daytime. In June, the westerly circulation weakened and its southern branch retreated gradually from the area, northerly weakened consequently, and southerly occurred more, dominated progressively and often happened in the daytime. In July, the southern branch of the westerly circulation withdrew from Mount Everest region substantially and rendered stable by the north of 35°N. Wherefore, southerly was most, predominated exceedingly in the region (Fig. 6(a), (b)), and concentrated in the afternoon (Fig. 6(a)). Because of the geography and height of the AWS on Mount Everest, the frequency of wind direction and diurnal variation of wind speed were not only influenced by upper level wind, but also impacted by the diurnal variation of mountain-vale wind.

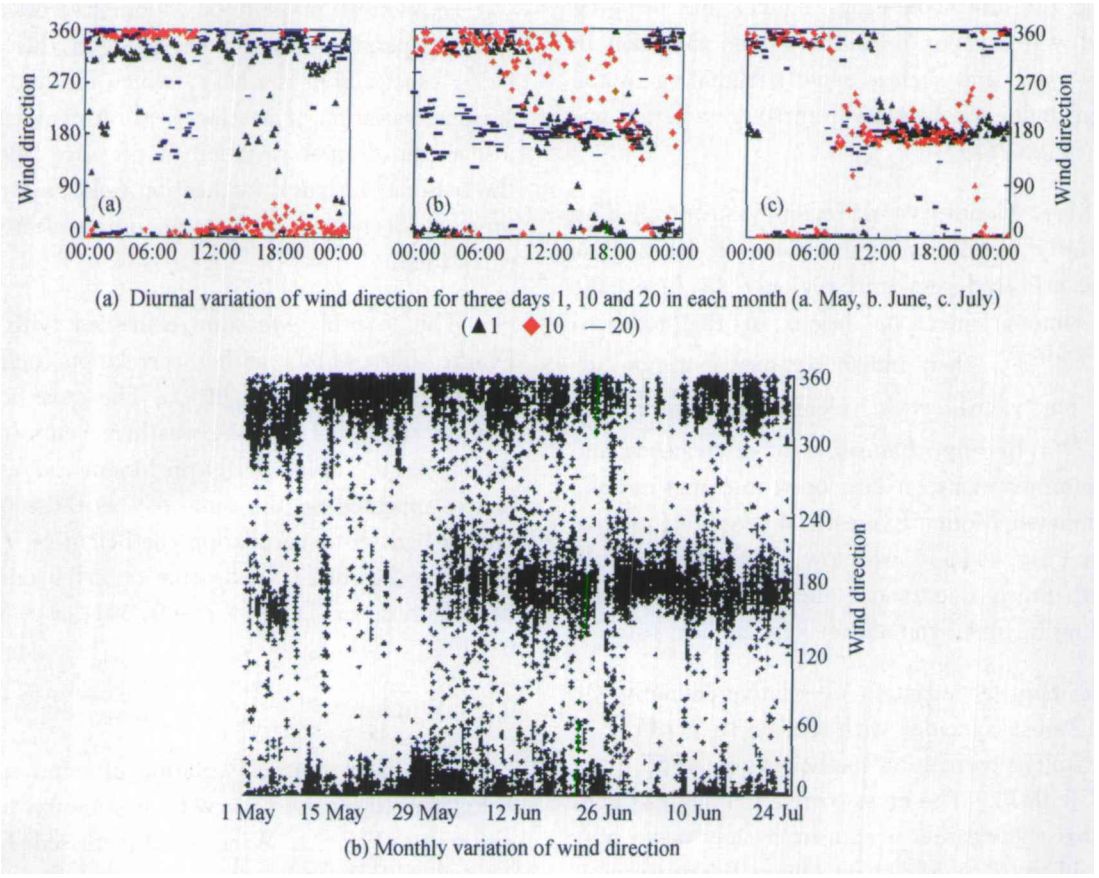

Fig. 6. Diurnal and monthly variation of wind direction on Mount Everest.

3 Discussion and conclusion

3.1 Averaged diurnal variation of meteorological elements on Mount Everest

The mean diurnal variation of air temperature was characterized by one peak and one vale, with the maximum at noon and minimum before sunrise. Relative humidity had the single-vale feature, with the minimum during sunrise. Air pressure was characterized by twin peaks and twin vales, with twin peaks at midnight and at noon, and twin vales before sunrise and after sundown. Wind speed was characterized by one peak with asymmetry during day and night, got

to maximum in the afternoon and kept low during the night to the next morning, southerly concentrated in the daytime, especially in the afternoon, and northerly predominated during the night.

3.2 Averaged monthly variation of meteorological elements on Mount Everest

The monthly meteorological features from May 1 to July 22 in 2005 are summarized in Table 2. For pressure and radiation, only the 10-minute mean value was available in the AWS. Therefore, we got the daily maximum and minimum from the 10-minute mean value in Table 2.

In May, Mount Everest region was controlled by the westerly circulation and influenced by airflow from the arid and semi-arid regions. All the meteorological elements fluctuated much, and northerly prevailed. In June, the Plateau summer monsoon began in the southern plateau, then Indian summer monsoon advanced northward, crossed the Himalayas, or moved northward through the Brahmaputra region and transferred westward, and entered into the Plateau's interior with plenty of water vapor[12,14,23]. Therefore, long-wave radiation, temperature, relative humidity and pressure increased, wind speed weakened, and wind direction turned from north to south. In July, Plateau summer monsoon and Indian summer monsoon developed into maturation and dominated in Mount Everest region substantially. So, all the meteorological elements had little rebounding, frequency of calm wind strengthened, and southerly dominated.

Table 2. Monthly average for daily mean, daily maximum and minimum of radiation (net radiation, DR, UR, DLR and ULR) ($W \cdot m^{-2}$), air temperature (℃), relative humidity (%), air pressure (hPa), wind speed ($m \cdot s^{-1}$), prevailing wind direction and its occurring frequency (%) on Mount Everest (6523 m a. s.l) from May 1 to July 22 in 2005

		Net radiation	Short-wave radiation		Long-wave radiation	
			DR	UR	DLR	ULR
May	Mean	36.87	396.98	276.41	169.34	253.04
	Max Mean	336.27	1363.97	936.43	243.81	297.84
	Min Mean	−109.39	−4.87	−0.16	128.29	219.78
June	Mean	49.70	373.83	255.36	212.69	281.46
	Max Mean	397.83	1341.57	876.14	294.32	323.85
	Min Mean	−100.33	−4.81	−0.02	162.82	245.42
July (1 to 22)	Mean	49.17	306.10	243.71	283.02	296.24
	Max Mean	332.09	1352.59	1015.37	333.50	332.50
	Min Mean	−54.83	−3.67	−0.83	231.34	265.80
		Air temperature (℃)	Relative humidity (%)	Air pressure (hPa)	Wind speed ($m \cdot s^{-1}$)	Prevailing Wind direction (occurring frequency)
May	Mean	−10.75	44.56	456.15	7.52	Northerly (30.1%) North-north-westerly (26.5%)
	Max Mean	−6.03	75.04	457.37	18.77	
	Min Mean	−15.39	18.40	454.93	0	
June	Mean	−5.1	65.78	458.97	3.18	Southerly (22.5%) Northerly (15.6%)
	Max Mean	−0.26	91.50	459.99	11.13	
	Min Mean	−9.38	32.50	458.09	0	
July (1 to 22)	Mean	−3.25	86.02	461.08	2.23	Southerly (29.8%) Calm wind (15.4%)
	Max Mean	3.92	94.97	462.00	7.27	
	Min Mean	−7.00	59.35	460.26	0	

Notes: In this Table, Mean stands for total mean of 10-minute mean observational values, Max Mean for the mean value of daily maximum, and Min Mean for the mean of daily minimum. DR stands for downward short-wave radiation, UR for upward short-wave radiation, DLR for downward long-wave radiation, ULR for upward long-wave radiation

3.3 Comparison of monthly variation between Mount Everest and Dingri

Influenced by the same atmosphere circulation, Mount Everest (Fig. 4(a)) and Dingri County (Fig. 4(b)) had the similar monthly variation of meteorological features from May 1 to July 22, 2005, with the correlation coefficient of 0.928 for daily mean

temperature, 0.877 for minimum temperature, 0.682 for maximum temperature, 0.755 for relative humidity, 0.826 for pressure and 0.676 for wind speed. Furthermore, all the correlation was significant at the 0.001 level ($n = 83$). For daily mean, minimum and maximum temperature, the vertical mean gradient was 0.75℃/100 m, 0.63℃/100 m, and 0.82℃/100 m, respectively. The vertical maximum gradient was 0.85℃/100 m, 0.83℃/100 m and 1.18℃/100 m, respectively. The vertical minimum gradient was 0.55℃/100 m, 0.43℃/100 m and 0.43℃/100 m, respectively.

The cross-correlation analysis (Fig. 5) suggested that most weather events on Mount Everest prominently appeared on the same day as those on Dingri, especially those from daily mean pressure (Fig. 5(e)), temperature (Fig. 5(a)) and relative humidity (Fig. 5(d)) with the cross-correlation coefficient of 0.673, 0.485 and 0.487 ($n = 83$, $p < 0.001$), respectively. However, some weather events on Mount Everest lagged one day behind those on Dingri, such as those from daily mean pressure, daily minimum and maximum temperature, although the cross-correlation coefficient was rather lower (0.341, 0.366, 0.245, respectively).

Comparing figures 5(a), 5(b), 5(c), 5(d), 5(e), 5(f), the cross-correlation coefficient from pressure was the highest, while the coefficient from wind speed and maximum temperature was the lowest, which was due to the local influence in Dingri County, such as huge buildings, human activities, etc. on wind speed and maximum temperature. However, the local influence had less effect on pressure. Therefore, forecasting weather events on Mount Everest from pressure on Dingri was more reliable than those from the other meteorological elements.

The observational period was rather short only from May 1 to July 22 in 2005. Wherefore, to substantiate the view, more observational programmes and investigations are needed in the future.

Acknowledgements We extend our much gratitude to all the crews of 2005 integrated scientific expedition to Mount Everest for their hard fieldwork, especially to Dr. Tang Shulin for establishing and maintaining the AWS, and to Duan Jianping for measuring site of the AWS. We give special thanks to He Yong for providing the meteorological data of Dingri County. Thanks also go to Cui Xiaoqing, Xu Jianzhong, Du Wentao, Liu Weigang and all the crews in the expedition for their help in the fieldwork. Without their efforts and help, this work would not have been possible.

References

1 Barros AP, Kim G, Williams E, et al. Probing orographic controls in the Himalayas during the monsoon using satellite imagery. Nat Hazards Earth Syst Sci, 2004, 4: 29—51
2 Bollasina M and Benedict S. The role of the Himalayas and the Tibetan Plateau within the Asian monsoon system. Bull Am Meteorol Soc, 2004, 85(7): 1001—1004
3 Venables S. Everest summit of achievement. R Geogr Soc London, 2003, 252
4 Egger J, Bajrachaya S, Egger U, et al. Diurnal winds in the Himalayan Kali Gandaki Valley. Part I: Observations. Mon Wea Rev, 2000, 128: 1106—1122
5 West JB. Barometric pressures on Mt. Everest: New data and physiological significance. J Appl Physiol, 1999, 86: 1062—1066
6 Huey RB and Eguskitza X. Limits to human performance: Elevated risks on high mountains. J Exp Biol, 2001, 204: 3115—3119
7 Tibetan Scientific Expedition Team from Chinese Academy of Sciences. Report on scientific expedition to Mount Everest region: 1966—1968. In: Meteorology and Radiation (in Chinese). Beijing: Science Press, 1975a
8 Tibetan Scientific Expedition Team from Chinese Academy of Sciences. Report on scientific expedition to Mount Everest region: 1966—1968. In: Physical Geography (in Chinese). Beijing: Science Press, 1975b
9 Bertolani L, Bollasina M and Tartari G. Recent biennial variability of meteorological features in the Eastern Highland Himalayas. Geophys Res Lett, 2000, 27: 2185—2188
10 Moore GWK and Semple JL. High Himalayan meteorology: Weather at the South Col of Mount Everest. Geophys Res Lett, 2004, 31: L18109
11 Egger J, Bajrachaya S, Heinrich R, et al. Diurnal winds in the Himalayan Kali Gandaki valley. Part III: Remotely piloted aircraft soundings. Mon Wea Rev, 2002, 130: 2042—2058
12 He H, McGinnis JW, Song Z, et al. Onset of the Asian monsoon in 1979 and the effect of the Tibetan Plateau. Mon Wea Rev, 1987, 115: 1966—1995
13 Barros AP and Lang TJ. Monitoring the monsoon in the Himalayas: Observations in Central Nepal, June 2001. Mon Wea Rev, 2003, 131: 1408—1427
14 Qin D, Hou S, Zhang D, et al. Preliminary results from the chemical records of an 80.4 m ice core recovered from East Rongbuk Glacier, Qomolangma (Mount Everest). Ann Glaciol, 2002, 35: 278—284
15 Ren J, Qin D, Kang S, et al. Glacier variations and climate warming and drying in the central Himalayas. Chin Sci Bull, 2004, 49: 65—69
16 Ren J, Jing Z, Pu J, et al. Glacier variations and climate change in the central Himalayas over the past few decades. Ann Glaciol, 2006, 43: 218—222
17 Kang S, Mayewski PA, Qin D, et al. Seasonal differences in snow chemistry from the vicinity of Mount Everest, central Himalayas. Atmos Environ, 2004, 38: 2819—2829
18 Hou S, Qin D, Zhang D, et al. Comparison of two ice core chemical records recovered from the Qomolangma (Mount Everest) region. Ann Glaciol, 2002, 35: 266—272
19 Thompson LG, Yao T, Mosley-Thompson, et al. A high-resolution millennial record of the south Asian monsoon from Himalayan ice cores. Science, 2000, 289: 1916—1919
20 IPCC. Climate Change 2001. The Science Basis, Contribution of Work Group I to Third Assessment Report of the Intergovernmental Panel on Climate Change. Cambridge-New York: Cambridge University Press, 2001, 882

21 IPCC. Climate Change 2001. Impact, Adaptation, and Vulnerability. Contribution of Work Group II to Third Assessment Report of the Intergovernmental Panel on Climate Change. Cambridge-New York: Cambridge University Press, 2001, 1032
22 Zhou S. Meteorology and Climatology (in Chinese). 3rd Ed. Beijing: China Higher Education Press, 1999, 21—117
23 Ye D and Gao Y. Meteorology of the Tibetan Plateau (in Chinese). Beijing: Science Press, 1979, 10—262
24 Gong Y, Duan T, Chen L, et al. The variation characteristics of radiation budget components of the western Tibetan plateau in 1997/1998. Acta Meteorologica Sinica (in Chinese), 2005, 63: 225—235
25 Ma P, Zhang Q, Yang X, et al. Characteristics of maximum and minimum temperature variation in near surface layer. Meteorological Science and Technology (in Chinese), 2006, 34: 83—87
26 Li Z and Luo P. SPSS for Windows—Windows Tutorial for SPSS Statistical Analysis (in Chinese). 2nd Ed. Beijing: Electronic Industry Press, 2003, 463—464